Journal of Inorganic and Organometallic Polymers and Materials (2024) 34:1609–1619
https://doi.org/10.1007/s10904-023-02901-8

RESEARCH

First-Principles Calculations of Novel Lead-Free X_2GeSnI_6 (X = Rb, Cs) Double Perovskite Compounds for Optoelectronic and Energy Exploitations

Malak Azmat Ali[1] · M. Musa Saad H.-E.[2] · Ammar M. Tighezza[3] · Shaukat Khattak[4] · Samah Al-Qaisi[5] · Muhammad Faizan[6]

Received: 10 August 2023 / Accepted: 5 October 2023 / Published online: 4 November 2023

Abstract

We investigate the structural, optoelectronic, and thermoelectric properties of halide double perovskite X_2GeSnI_6 (X = Rb, Cs) compounds employing the full potential linearized augmented plane wave approach within the framework of density functional theory. The negative formation energies and positive phonon frequencies indicate their structural and dynamical stabilities. The density of states and band structures were estimated while utilizing Tran and Blaha-modified Becke-Johnson (TB-mBJ) potential as exchange–correlation approximation. The electronic structure calculation show direct bandgaps of 0.49 eV for Rb_2GeSnI_6 and 0.57 eV for Cs_2GeSnI_6, suggesting semiconducting behavior. To establish their use in photovoltaic and optoelectronic devices, we compute the optical properties of the compounds. Furthermore, the thermoelectric characteristics such as electrical conductivity, Seebeck coefficient, thermal conductivity, and figure of merit, have been studied in the temperature range of 100 to 800 K. Both materials exhibit positive Seebeck coefficient, indicating the materials to be p-type semiconductors. The examined thermoelectric properties of both the compounds imply their potential use in thermoelectric devices.

Keywords Double perovskites · Semiconductors · Optical properties · Thermoelectric properties · Photovoltaic applications

1 Introduction

The need for energy has accelerated efforts to develop unconventional and non-fossil fuel energy sources. Consequently, renewable energy sources are given more attention globally [1, 2]. Renewable energy can be produced by exploiting the thermoelectricity that enables the effective use of waste heat by transforming thermal energy to electrical power [3, 4]. The figure of merit (ZT) establishes the capabilities of thermoelectric materials. A desired ZT is characterized by high electrical and low thermal conductivities [5]. Besides thermoelectricity, solar cells also play a vital role in renewable energy applications [6]. In this context, interest has been developed into the perovskite-based compounds after it was found that they display reasonable thermoelectric and optical properties. Due to their wide range of physical, chemical, and catalytic properties, they have garnered great attention of the research community [7–17]. Simple perovskite (ABX_3) has a cubic crystal shape with the Fm-3m space group. The cation residing on site A and combined with its neighbors generates 12-fold cuboctahedron geometry because of having 12 coordination numbers.

✉ Malak Azmat Ali
azmatupesh@gmail.com

[1] Department of Physics, Government Post Graduate Jahanzeb College Saidu Sharif, Swat 19130, Khyber Paktunkhwa, Pakistan

[2] Department of Physics, College of Science and Arts in Al-Muthnib, Qassim University, 51931 Al-Muthnib, Saudi Arabia

[3] Department of Chemistry, College of Science, King Saud University, P. O. Box 2455, 11451 Riyadh, Saudi Arabia

[4] Department of Physics, Abdul Wali Khan University, Mardan 23200, Pakistan

[5] Palestinian Ministry of Education and Higher Education, Nablus, Palestine

[6] College of Materials Science and Engineering, Jilin University, Changchun 130012, China

Octahedral geometry is produced by the interaction of the cation lying on B-site with its surroundings [8]. Thanks to their promise for applications in modern science, double perovskites in addition to the simple perovskites have stimulated a lot of research work [18, 19]. They are represented by the formula of $A_2BB'X_6$, where X can be an oxide or a halide, B and B′ sites can reside transitional or non-transitional cations, and a rare-earth or alkaline-earth metal resides on the A site [20]. Recent research on some double perovskites has revealed important information about their optoelectronic and transport capabilities [21–24].

Recently, a wide range of distinctive double perovskite compounds has been studied. In this context, detailed descriptions of A as K, Cs, Rb, B^+ cation as Cu, Ag, In, Ge, B^{3+} cation as Bi, Sb, Sn and X as Cl, Br, I compounds were provided, showing their optoelectronics and transport capabilities [25–29]. McClure et al. [30] have proposed $Cs_2AgBiCl_6$ and $Cs_2AgBiBr_6$ as potential non-toxic replacements for lead-based perovskites. Long carrier lifetimes and bandgap energy have been observed in the visible spectrum for $Cs_2AgBiBr_6$. Berri and Bouarissa [31] explored K_2XBF_6 (X = Na, Ag,; B = Pd, Rh, Nb, Ni, Ti, Ru) as high ZT double perovskites. Ali et al. [29] calculated direct bandgaps for $Rb_2GeSnCl_6$ and $Rb_2GeSnBr_6$ as 1.2961 and 0.799 eV, respectively. They suggested these materials for energy based applications. Houari et al. [8] studied structural, electronic and optical properties of K_2GeSnX_6 (X = Br, I) and calculated high absorption coefficients for these perovskites. They recommended these materials for solar cell applications. Mukkadar and Ghosh [18] found that $Cs_2GeSnCl_6$ based hetrojuction solar cells are 16.35% efficient. Behera and Mukherjee [32] calculated bandgaps of $Cs_2GeSnCl_6$ and $Cs_2GeSnBr_6$ as 1.37 and 0.91 eV, respectively. They reported excellent optical and thermoelectric properties of these double halide perovskites.

A review of the literature revealed that halide double perovskites X_2GeSnI_6 (X = Rb, Cs) have not yet been substantially studied. This has triggered this study, which used first-principles simulations to examine the structural, electrical, optical, and thermoelectric properties of X_2GeSnI_6 compounds. The manuscript is divided into three portions. The introduction is covered in Part 1, the computational approach utilized in the current study is described in depth in Part 2, and the results and conclusions are covered in Sect. 3. An in-depth analysis of the estimated optical and thermoelectric properties of the examined compounds reveals applications for solar cells and other energy-producing devices.

2 Computational Details

The physical properties of X_2GeSnI_6 (X = Rb, Cs) compounds are examined in this study using the full potential linearized augmented plane wave (FP-LAPW) technique as implemented in the WIEN2k code [33] based on density functional theory (DFT) [34]. The Kohen-Sham equations were solved using the gradient generalized approximation GGA in the form of the Perdew-Burke-Ernzerhof (PBE) exchange–correlation functional [35]. The optimization employed the PBE-GGA approximation, which provided accurate ground state values but underestimated the electronic properties. For bandgap precision, we also successfully used the modified Becke and Johnson potential (TB-mBJ) [36]. For the convergence criterion, RMT K_{max} is set to 7.0, where R_{MT} is the muffin-tin radius for the reciprocal lattice vector and K_{max} is the plane wave cut-off. The charge density's maximum Fourier expansion was set at $G_{max} = 12a.u.^{-1}$. The $10 \times 10 \times 10$ grid and a total of 1000 k-points were used to integrate the reciprocal space of the irreducible Brillouin zone. The self-consistent computations were carried out with total convergence threshold energy of 10^{-5} Ry for these materials. To ascertain the thermoelectric properties, we used the BoltzTraP simulation package [37]. For calculating the transport properties, a fine grid mesh ($46 \times 46 \times 46$) was considered. The phonon calculations have been carried out using CASTEP code with help of finite displacement technique [38].

3 Results and Discussion

3.1 Stability Aspects

According to the structural analysis of Rb_2GeSnI_6 and Cs_2GeSnI_6, these compounds crystallize in cubic symmetry with space group of Fm-3m, and the atomic positions that make up its unit cell are X (0.25, 0.25, 0.25), Ge (0, 0, 0), Sn (0.5, 0.5, 0.5), and I (0.25,0, 0). Figure 1 shows the structure of the X_2GeSnI_6 unit cell where (X = Rb, Cs).

The thermodynamic stability of these structures has been exploited by calculating the formation energies per atom (H_F) via Eq. 1 [39].

$$H_F = \frac{E_o - 2E_X - E_{Ge} - E_{Sn} - 6E_I}{10} \quad (1)$$

where, *Eo* is the total grond state energy of a X_2GeSnI_6 compound, and EX, EGe, ESn and EI are the energies of Rb/Cs, Ge Sn and I, respectively in bulk form. All these values are given in Table 1. This Table depict that the HF per atom for both the X_2GeSnI_6 compounds are negative. These negative values reflect that formation reaction for both the compounds is exothermic, therefore, the compounds are thermodynamically stable as per criteria [40].

The dynamical stability of both the X_2GeSnI_6 compounds was inspected by calculating the phonons bands as shown in Fig. 2. Where, the imaginary (negative)

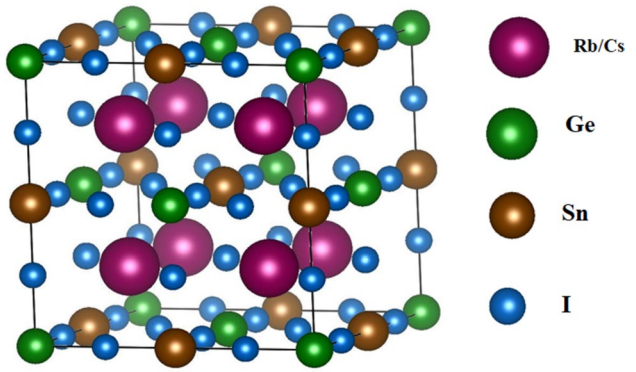

Fig. 1 The unit cell structure of double perovskites X_2GeSnI_6 (X = Rb, Cs)

frequencies are absent throughout the considered Brillion Zone. Therefore, the existence of only positive phonos frequencies confirm that both the studied compounds are dynamically stable [41]. Further, the empty spaces for phonons band within 4–5 THz are validated by considerable difference of atomic masses within X_2GeSnI_6 compounds. The lighter atom vibrates at a higher frequency than heavier atom, producing a gap between different phonon bands [42].

3.2 Structural Parameters

The optimized energy (eV) values are displayed against the volume in Fig. 3 where the PBE-GGA approximation was utilized to optimize the lattice parameters to make the structure appropriate and strain-free. The Murnaghan-equation-of-states (Eq. 2) [43] fit indicates that the highest amount of energy is released at the points when volume is minimal. The parameters given in Table 2 were obtained from this fit. As indicated from this Table, the computed lattice constants for Rb_2GeSnI_6 and Cs_2GeSnI_6 are $a_0 = 12.28$ and 12.22 Å, respectively. By substituting Cs for Rb, the atomic radii increase from 1.72 (Rb) to 1.88 (Cs), increasing the lattice constant. As a result, the inter atomic distance increases, making the material comparatively less dense and less solid, which results in a fall in the bulk modulus (B) value from 16.86 to 16.59 GPa. The bulk modulus of Cs_2GeSnI_6 is considerable, indicating that it is stiffer than Rb_2GeSnI_6. The change in the a_0 and B with cation/anion change has been also reported for other related halide double perovskites [29, 44].

3.3 Electronic Properties

Understanding a material's band gap is crucial for understanding it's optical and charge carrier properties. Figure 4

Table 1 Elemental (E_X, E_{Ge}, E_{Sn}, E_I) in bulk, total (E_o) and formation energies of X_2GeSnI_6 (X = Rb, Cs)

Perovskite	E_X	E_{Ge}	E_{Sn}	E_I	E_o	H_f
Rb_2GeSnI_6	− 81,095.65	− 57,091.71	− 168,069.63	− 193,637.96	− 1,549,199.39	− 2.60
Cs_2GeSnI_6	− 211,895.62	− 57,091.71	− 168,069.63	− 193,637.96	− 1,810,798.73	− 1.84

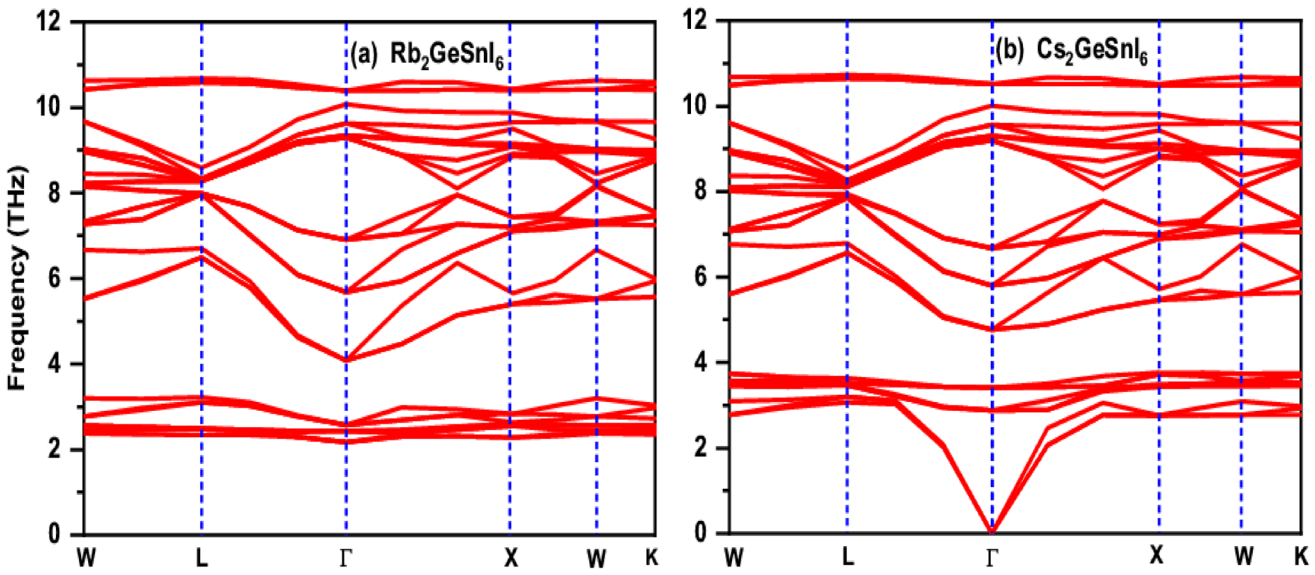

Fig. 2 Phonons band structures for **a** Rb_2GeSnI_6 and **b** Cs_2GeSnI_6

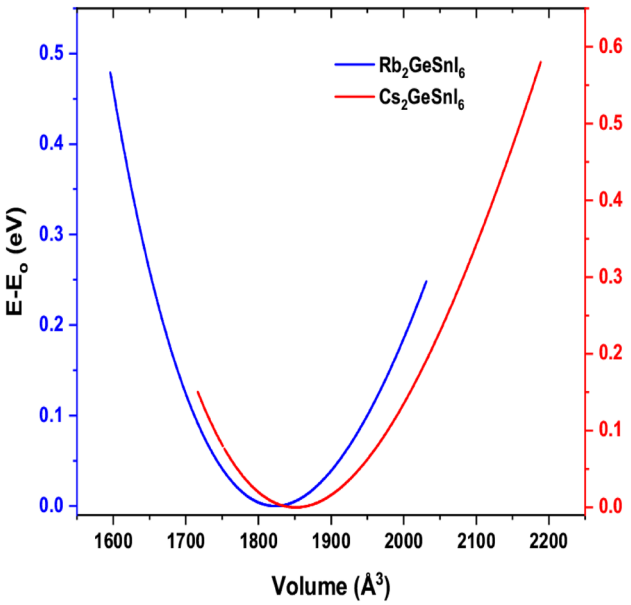

Fig. 3 Birch Murnaghan fit to the volume optimization of X_2GeSnI_6 (X = Rb, Cs)

Table 2 The calculated lattice constant (a_0) in (Å), Bulk modulus (B) in (Gpa), Volume in ($Å^3$), the derivative of bulk modulus ($B^{/}$), and band gap energy (eV) for X_2GeSnI_6 (X = Rb, Cs)

Compound	a_0 (Å)	B (GPa)	V ($Å^3$)	$B^{/}$	E_g(eV)
Rb_2GeSnI_6	12.22	16.86	1823.07	5.0	0.49
Cs_2GeSnI_6	12.28	16.59	1851.24	5.0	0.57

depicts the band structures estimated for Rb_2GeSnI_6 and Cs_2GeSnI_6, where, the maxima of the valence band and minima of the conduction band are located at the same symmetric point, indicating that the material under study is a direct band gap material. For Rb_2GeSnI_6 and Cs_2GeSnI_6, the calculated band gaps are 0.49 and 0.57 eV, respectively. For the optoelectronic application of a material operating in the visible and ultraviolet range, the band gap values of the material in this range are crucial. In addition to this, the fact that there is many more density levels in the conduction band than in the valence band indicates that the bulk of charge carriers in the conduction band are electrons.

Understanding the nature of the excitation of electrons from the valence band to the conduction band requires knowledge of a material's density of states (DOS). To better understand the band structure when closely inspected, the density of states (DOS) is studied in between − 8 and 8 eV energy range as shown in Fig. 5. The Fermi energy level (E_F), which is in the middle and has an energy value of 0 eV, divides the DOS-calculated plots into two parts. The valence band is the region to the left of the Fermi level, and the conduction band is the region to the right of the Fermi level.

In Fig. 5a and b, the DOS of Rb/Cs, Ge, Sn, and I are calculated and displayed in detail. Where, it is clear that s states of Sn make up the majority of the states contributing to the valence band at the E_F, with p states of Ge and the halogen ion I making up the minority. The s states of Ge and Sn, the halogen ions I, and the p states of Ge and Sn all contribute to a lesser extent to the valence band, overall. The highest contribution comes from the p states of I. Similarly in the conduction band, the calculation shows that the p states of Ge and Sn contribute the most along with d states of Rb/Cs, while s, and p states of Rb/Cs, s, and d sates of Ge and all the s, p, d state of I contribute the least.

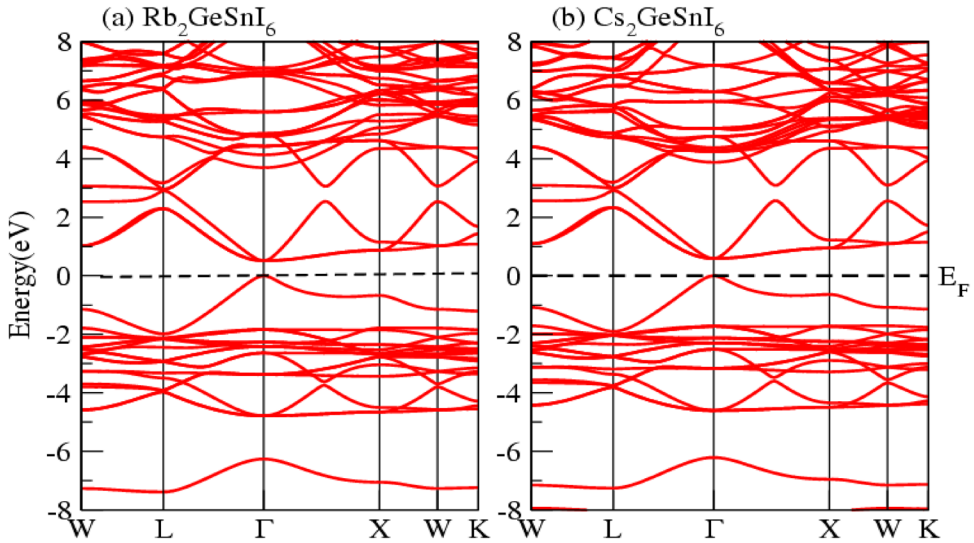

Fig. 4 Band structure plots for **a** Rb_2GeSnI_6 **b** Cs_2GeSnI_6

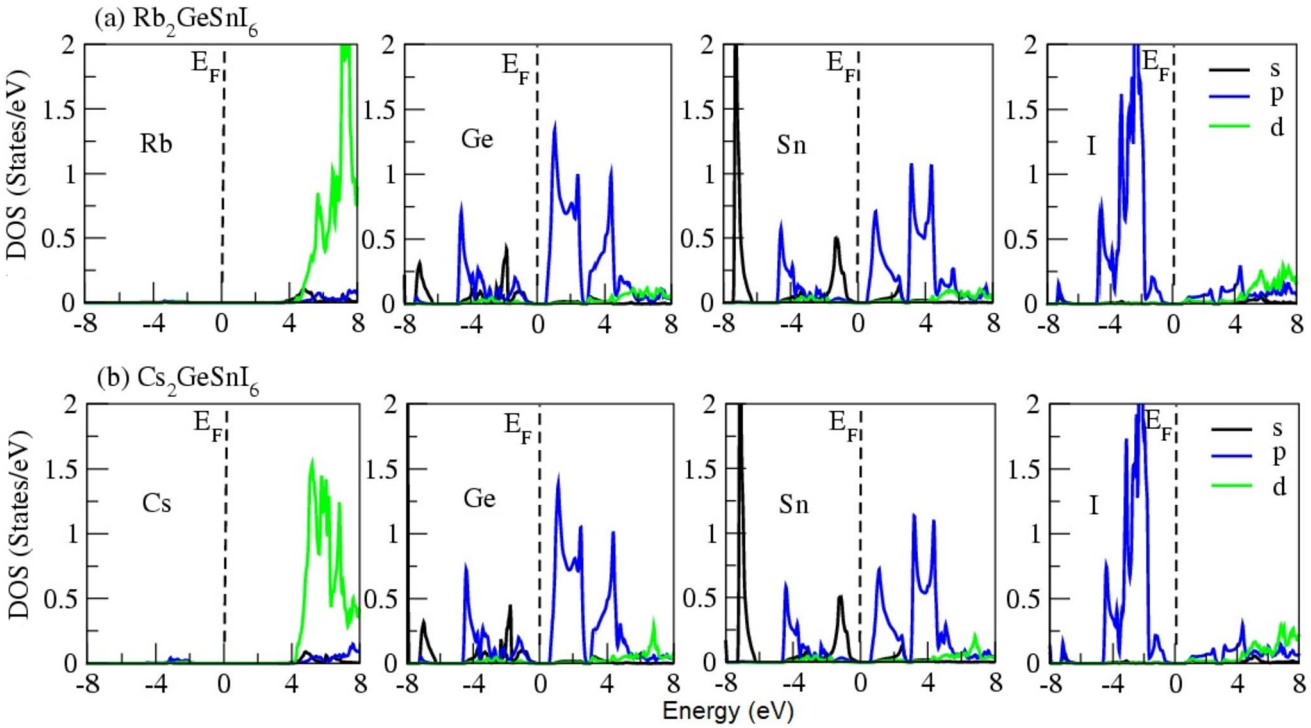

Fig. 5 Density of states (DOS) plots for **a** Rb_2GeSnI_6 **b** Cs_2GeSnI_6

3.4 Optical Properties

The choice of a material for an optoelectronic application is greatly influenced by the material's optical characteristics, which explain how a material behaves when it interacts with incident photons. Regarding optical applications, there are two primary types of materials: anisotropic and isotropic materials. When light is incident on a material from multiple directions, the properties of an isotropic material stay constant, whereas an anisotropic material exhibits varied qualities depending on the direction of the light. Knowing a photon's interaction with X_2GeSnI_6 (X = Rb, Cs) is required to predict their optical behavior. Calculations for both the inter-band and intra-band transitions are required for this work, but for optical properties, the inter-band transition is regarded as being more important than the intra-band transition since it plays a crucial part in photon absorption and emission [45, 46]. Figure 6 shows the real part, $\varepsilon_1(\omega)$, and imaginary part, $\varepsilon_2(\omega)$, of dielectric constant. $\varepsilon_1(\omega)$, shows the polarization behavior when the electric field of electromagnetic waves incident on a medium with different values of the refractive indices. A material medium's density affects the speed of light there, and different medium densities have varying refractive indices. The speed of light is greatest in a vacuum. In all other material mediums, the speed of light decreases with increasing material density and is the slowest in the medium with the highest density [47]. When the frequency of incident light is somewhat different from the resonance frequency, the polarization of incoming light dramatically reduces, and the absorption of incident light's energy starts. This is demonstrated by the imaginary component of the dielectric constant, or $\varepsilon_2(\omega)$, in Fig. 6b. Additionally, when the cation, X is altered, the values for the real and imaginary parts of the dielectric constant changes. Rb_2GeSnI_6 and Cs_2GeSnI_6 are low bandgap perovskites. Materials with such bandgap energies are important for capturing solar energy. Because, it can be seen from the figure that maximum of $\varepsilon_2(\omega)$ occur in the visible region.

Optical conductivity (σ) is defined as the measure of the incident photon's energy per unit length. According Fig. 7a, the Rb_2GeSnI_6 and Cs_2GeSnI_6 start to exhibit optical conductance when the energy of an incident photon is 0.49 and 0.57 eV, respectively. σ show sudden maximum values near 2 eV for both the perovskites. This signifies that Rb_2GeSnI_6 and Cs_2GeSnI_6 can be utilized for solar cells and other optical devices working the visible range of electromagnetic spectrum. Below 2 eV, and beyond 3.2 eV, σ exhibits small values. This means that in infrared and ultra violet regions, the optical conductance through X_2GeSnI_6 compounds is not effective, comparatively.

The quantity of light energy that scatters after striking a material's surface is measured by its reflectivity, $R(\omega)$. In Fig. 7b, the computed $R(\omega)$ of the compounds is displayed. For Rb_2GeSnI_6 and Cs_2GeSnI_6, their maximum

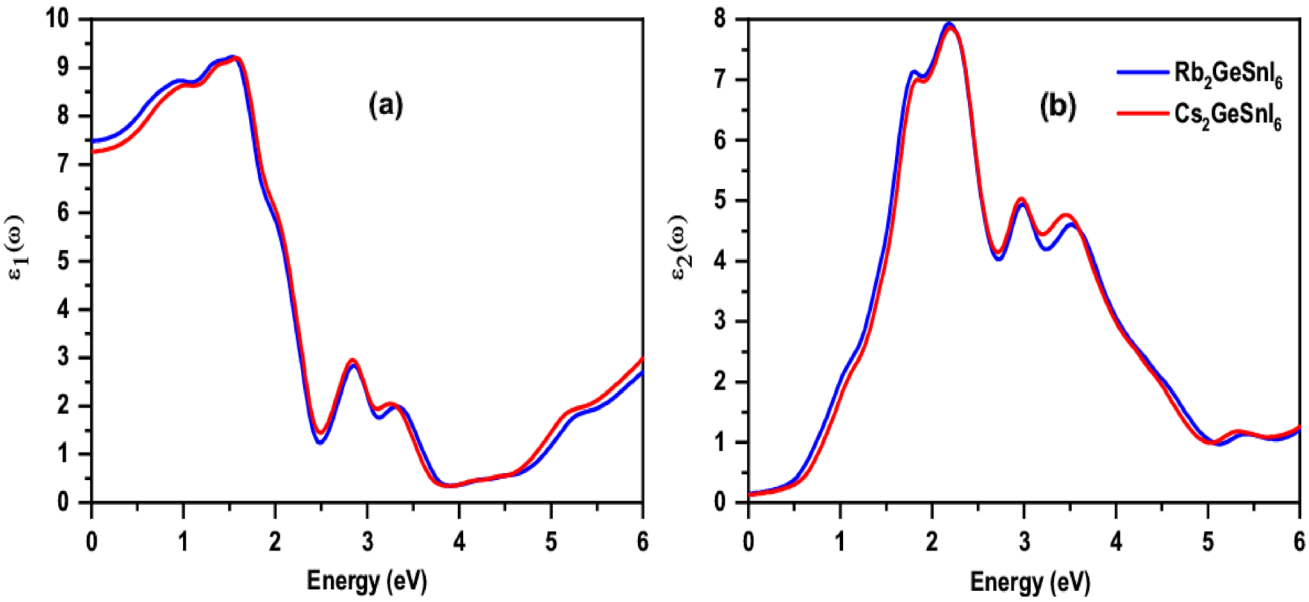

Fig. 6 Calculated **a** real, ε_1 (ω), **b** imaginary, ε_2 (ω) parts of the dielectric function of X_2GeSnI_6 (X = Rb, Cs)

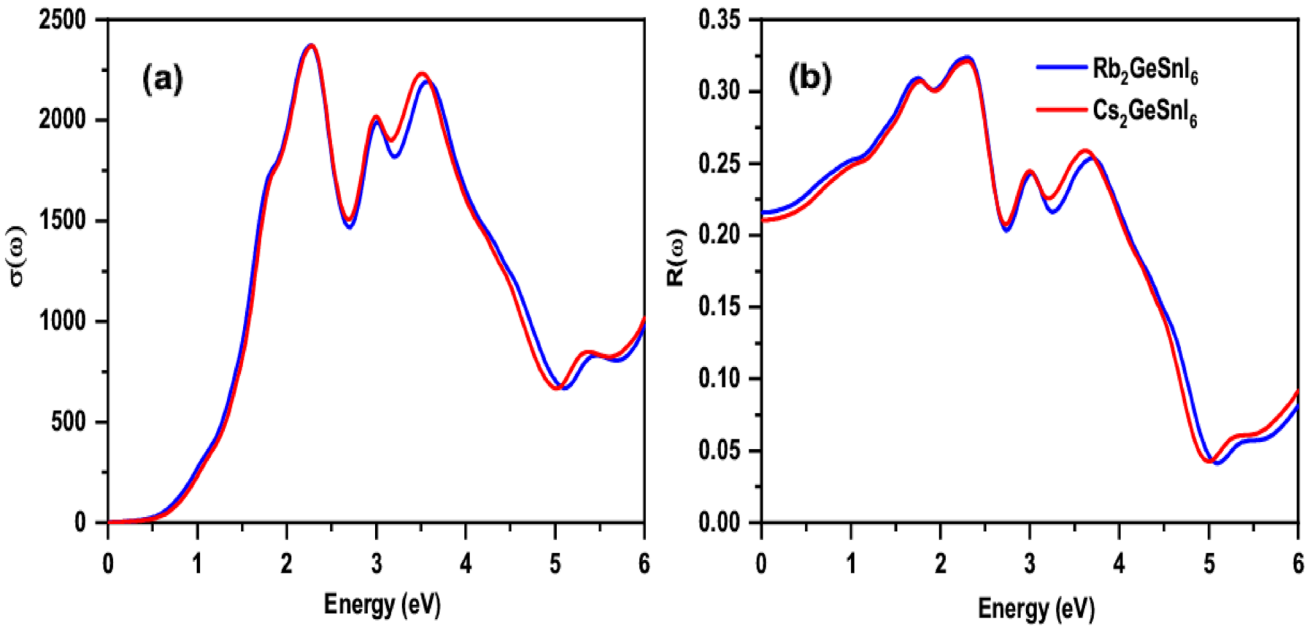

Fig. 7 Calculated **a** optical conductivity, σ (ω) and **b** reflectivity R (ω) for X_2GeSnI_6 (X = Rb, Cs)

values were found to be 0.318 and 0.325, respectively. The highest loss of energy happens at the location where the value of reflectivity R(ω) is maximum. Where, the static values R(ω) for both the compounds is nearly 020. Overall, the R(ω) has small values in studied energy range comparatively to other double perovskites [48].

3.5 Thermal Properties

The thermoelectric characteristics of X_2GeSnI_6 (X = Rb, Cs) were calculated using the BoltzTrap code based on classical Boltzmann transport theory (CBT) [29] in temperature range of 100–800 K and displayed in Figs. 9, 10, and 11. The both

the compounds were found stable in this temperature range from negative values of Gibbs free energy (Fig. 8) calculated through Gibbs2 code [49].

The migration of electrons and phonons is what causes a semiconducting material's thermal conductivity phenomena.

$$\kappa = \kappa_e + \kappa_L \tag{2}$$

where, the terms κ_e and κ_L refer to the electronic and lattice (phonon) thermal conductivities, respectively. These terms against temperature for the X_2GeSnI_6 compounds has been given in Fig. 9. The BoltzTraP code, which is based on the classical approach and has a limited application, cannot be utilized to calculate κ_L, therefore, κ_L has been calculated analytically through Slack equation [50]. Figure 9a shows that κ_e for both the double perovskites increases with temperature rise. This type of character is common in the semiconductors [5]. The maximum values of κ_e are reported as 0.351 and 0.353 W/mK for Rb_2GeSnI_6 and Cs_2GeSnI_6, respectively at 800 K. Overall, for both the perovskites, the values of κ_e are nearly same at lower and higher temperatures. Figure 9b explores the temperature dependent κ_L for the studied X_2GeSnI_6 compounds which show the opposite character to κ_e, κ_L decreases with rise in temperature. In the entire considered temperature range, both the compounds have almost same corresponding values of κ_L. This may be justified by nearly same bandgaps values for both the perovskites. The minimum calculated values of κ_L for Rb_2GeSnI_6 and Cs_2GeSnI_6 are 0.359 and 0.353 W/mK, respectively at 800 K.

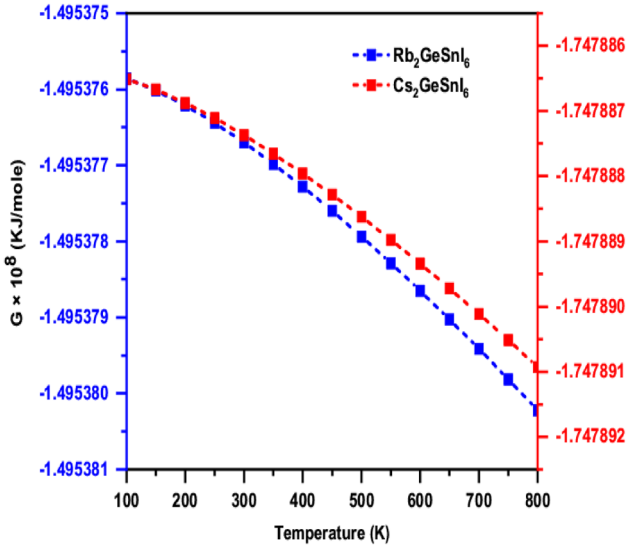

Fig. 8 The calculated Gibbs free energy (G) for Rb_2GeSnI_6 and Cs_2GeSnI_6 in temperature rang 100–800 K

The graphs of the electrical temperature (σ) vs. temperature for Rb_2GeSnI_6 and Cs_2GeSnI_6 are displayed in Fig. 10a. It counts the number of electrons and holes that are accessible to carry charge during the transmission of electrical energy. It has been noted that when temperature rises, electrical conductivity increases. The predicted σ for the double perovskites Rb_2GeSnI_6 and Cs_2GeSnI_6 are 157.78/183.61 × $(\Omega m)^{-1}$ at a temperature 100 K, and this value reaches a maximum of 470,029/5095.84 $(\Omega\ m)^{-1}$ at a temperature of 800 K. This is because at high temperatures, both free charge carriers (electron/hole) and their kinetic energy increase, leading to the dissolution of covalent bonds, the release of additional free charge carriers, and an increase in

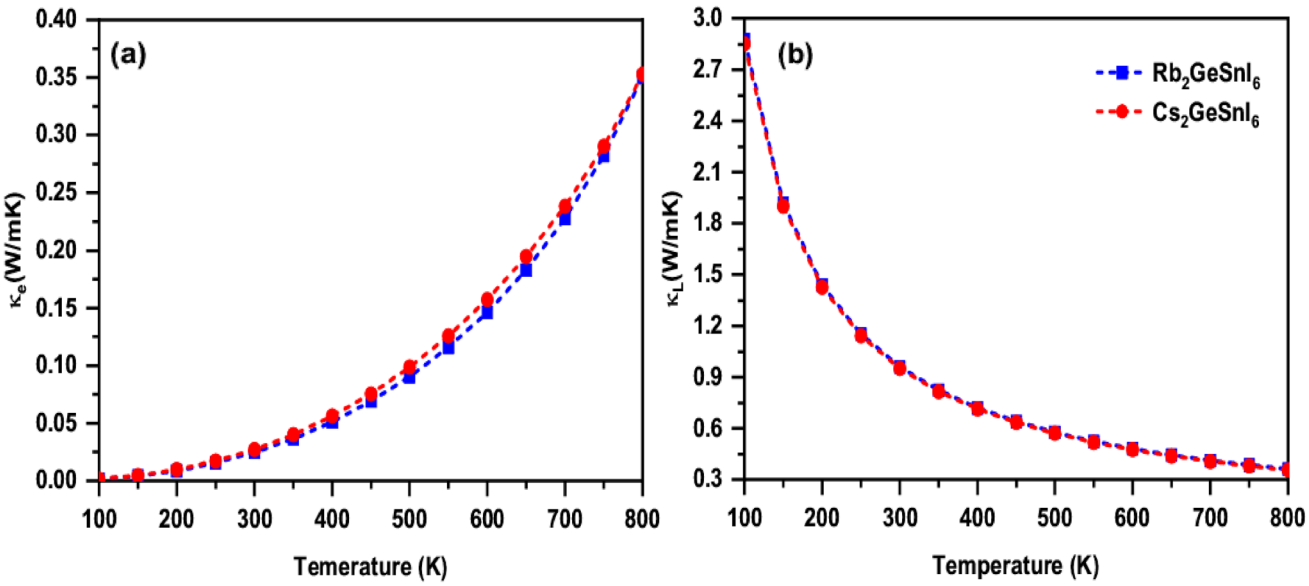

Fig. 9 **a** electronic, κ_e and **b** lattice, κ_L thermal conductivities of Rb_2GeSnI_6 and Cs_2GeSnI_6 in temperature rang 100–800 K

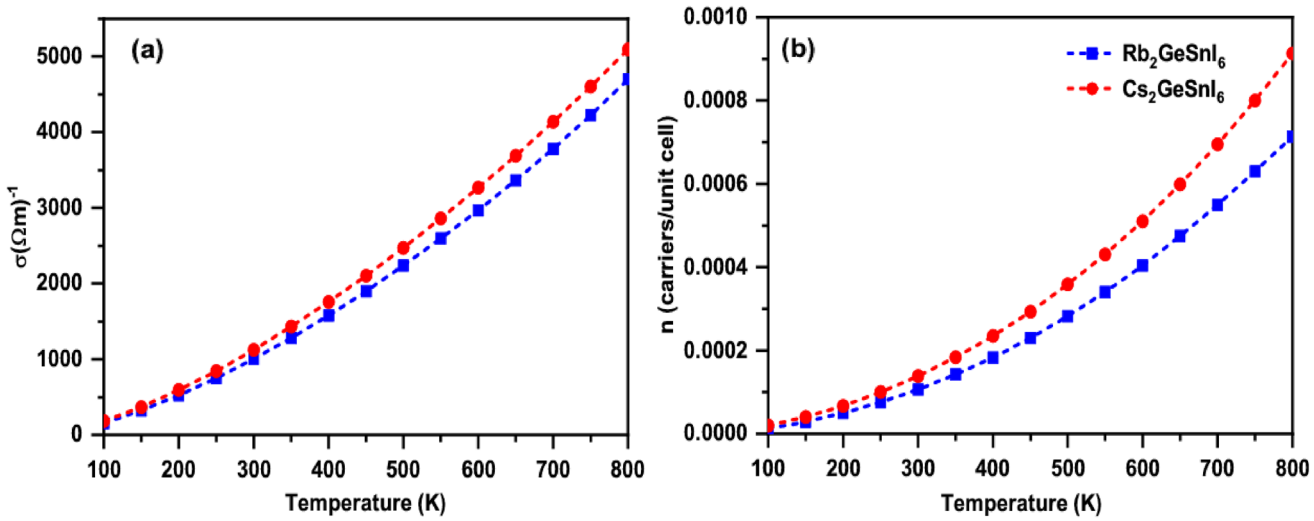

Fig. 10 Temperature dependent **a** electrical conductivity (σ) **b** carriers per unit cell (*n*) for Rb_2GeSnI_6 and Cs_2GeSnI_6

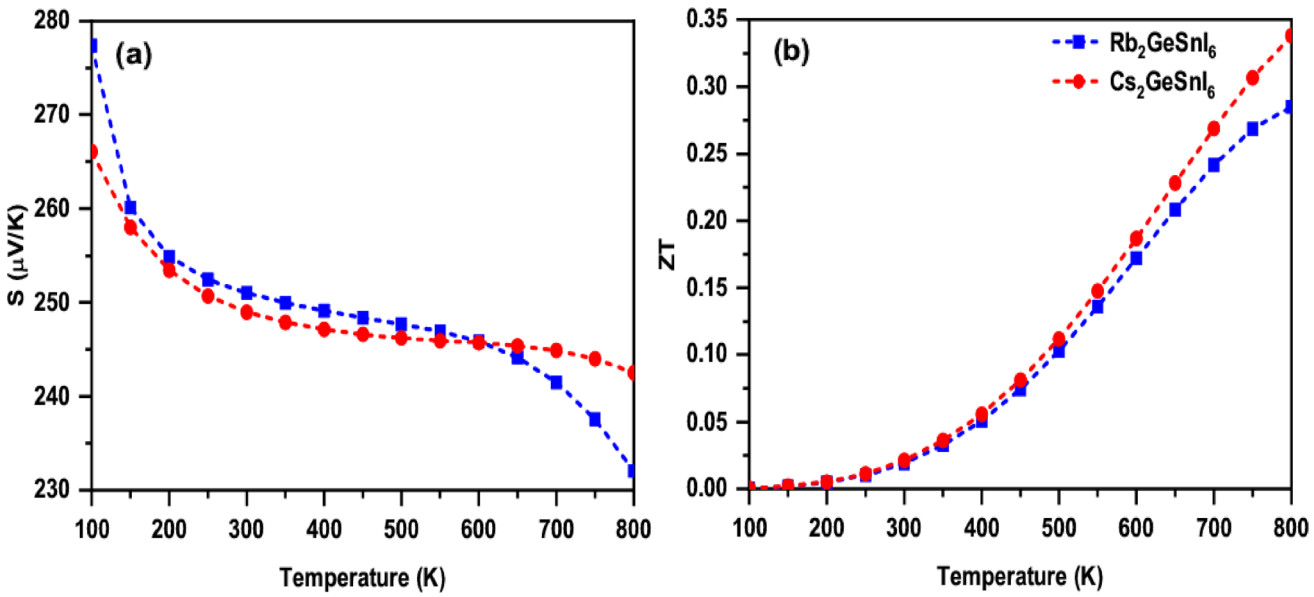

Fig. 11 **a** Seebeck coefficients (S) **b** Figure of merit (ZT) for Rb_2GeSnI_6 and Cs_2GeSnI_6 in temperature rang 100–800 K

conductivity. This phenomenon demonstrates the semiconducting nature of X_2GeSnI_6 (X = Rb, Cs). Due to fewer collisions, Cs_2GeSnI_6 has a higher electrical conductivity than Rb_2GeSnI_6. This can be justified from Fig. 10b. Where, the charge carriers per unit cell for Cs_2GeSnI_6 are greater than Rb_2GeSnI_6 and this trend is maintained in whole considered temperature range. Overall, the n values increases for each compound with rise in temperature. The increase in temperature free more charge carriers, therefore, n increases.

The Seebeck cofficients (S) indicate the potential difference due to temperature change. Figure 11a displays the computed values of the S. These values for the X_2GeSnI_6 perovskiets are positive, indicating that holes predominate as charge carriers and the materials under study are p-type semiconductors. For Rb_2GeSnI_6 and Cs_2GeSnI_6, the S values are 277.40 and 266.10 μV/K at 100 K, respectively. Following this, the S value drops for both the perovskites and Rb_2GeSnI_6 and Cs_2GeSnI_6 achieves a values of 232.07 and 242.54 μV/K, respectivelly at 800 K.

In the analysis of the thermoelectric efficiency of any given material, the figure of merit (ZT) is crucial [51, 52]. Because, it is the most important factor in determining how effectively a material's thermoelectric capabilities may be used in thermoelectric devices. Plotted against the temperature in Fig. 11b

are the computed values for the ZT. Where, the ZT values increases with the rise in temperature for both the X_2GeSnI_6 compounds, and attain a maximum values of 0.285/0.338 for Rb_2GeSnI_6/Cs_2GeSnI_6 at 800 K. These values are comparable to other related double perovskites [32].

4 Conclusions

Density functional theory has been used to explore the physical properties of double-perovskite X_2GeSnI_6 (X = Rb, Cs) compounds in this study. The studied compounds meet the stability criterion as backed by the negative formation energies and positive phonons frequencies. The investigated compounds are direct bandgap semiconductors with bandgap values of 0.49 and 0.57 eV, respectively. A thorough investigation of the optical parameters has been conducted to comprehend the optical properties. The outcomes of the calculations show that compounds have outstanding dielectric and excellent visible light absorption properties. Therefore, both the X_2GeSnI_6 double perovskites are suggested for solar cell applications. The calculated thermoelectric properties recommended these compounds as high temperature thermoelectric materials. Overall, the usage of these compounds in optical and thermoelectric devices is demonstrated by the proper values of predicted parameters, such as an adequate direct band gap, exceptional absorption spectra, and Seebeck coefficient.

Acknowledgements This work was supported by Researchers Supporting Project number (RSPD2023R765), King Saud University, Riyadh, Saudi Arabia

Author Contributions MAA: Investigation; visualization; calculations; writing original draft; Methodology; conceptualization; review and editing; MMSHE: review and editing; Investigation; Methodology; Resources; AMT: calculations; Methodology; Investigation; review and editing; Resources, Supervision; SK: writing original draft; Investigation; review and editing; Supervision; SAQ: conceptualization; Methodology; review and editing; MF: visualization; Software; review and editing.

Funding The authors have not disclosed any funding.

Data Availability The authors declare that the data supporting the findings of this study are available within the article.

Declarations

Conflict of interest The authors declare that they have no known competing financial interests or personal relationships that could have appeared to influence the work reported in this paper.

References

1. M.H. Elsheikh, D.A. Shnawah, M.F.M. Sabri, S.B.M. Said, M.H. Hassan, M.B.A. Bashir, M. Mohamad, A review on thermoelectric renewable energy: principle parameters that affect their performance. Renew Sustain. Energy Rev. **30**, 337 (2014)
2. X.F. Zheng, C.X. Liu, Y.Y. Yan, Q. Wang, A review of thermoelectrics research—recent developments and potentials for sustainable and renewable energy applications. Renew. Sustain. Energy Rev. **32**, 486 (2014)
3. J. Singh, T. Kaur, A.P. Singh, M. Goyal, K. Kaur, S.A. Khandy, I. Islam, A.F. Wani, R. Krisan, M.M. Sinha, S.S. Verma, LiNbCoX (X= Al, Ga) quaternary Heusler compounds for high-temperature thermoelectric properties: a computational approach. Bull Mater. Sci. **46**, 103 (2023)
4. P. Verma, C. Singh, P.K. Kamlesh, K. Kaur, A.S. Verma, Nowotny-Juza phase KBeX (X = N, P, As, Sb, and Bi) half-Heusler compounds: applicability in photovoltaics and thermoelectric generators. J. Mol. Model. **29**, 23 (2023)
5. S. Al-Qaisi, A.M. Mebed, M. Mushtaq, D.P. Rai, T.A. Alrebdi, R.A. Sheikh, H. Rached, R. Ahmed, M. Faizan, S. Bouzgarrou, M.A. Javed, A theoretical investigation of the lead-free double perovskites halides Rb_2XCl_6 (X = Se, Ti) for optoelectronic and thermoelectric applications. J. Comput. Chem. **44**, 1690 (2023)
6. M. Faizan, K.C. Bhamu, G. Murtaza, X. He, N. Kulhari, M.M. Al-Anazy, S.H. Khan, Electronic and optical properties of vacancy ordered double perovskites A_2BX_6 (A = Rb, Cs; B = Sn, Pd, Pt; and X = Cl, Br, I): a first principles study. Sci. Rep. **11**, 6965 (2021)
7. A.V. Andrianov, A.N. Aleshin, L.B. Matyushkin, Terahertz vibrational modes in $CH_3NH_3PbI_3$ and $CsPbI_3$ perovskite films. JETP Lett. **109**, 28 (2019)
8. M. Houari, B. Bouadjemi, A. Abbad, T. Lantri, S. Haid, S. Benstaali, M. Matougui, S. Bentata, Lead-free semiconductors with high absorption: insight into the optical properties of K2GeSnBr 6 and K2GeSnI6 halide double perovskites. JETP Lett. **112**, 364 (2020)
9. S. Kumari, P.K. Kamlesh, L. Kumari, S. Kumar, S. Kumari, R. Singh, R. Gupta, M.S. Chauhan, U. Rani, A.S. Verma, Progress in theoretical study of lead-free halide double perovskite Na2AgSbX6 (X = F, Cl, Br, and I) thermoelectric materials. J. Mol. Model. **29**, 195 (2023)
10. M. Rani, P.K. Kamlesh, S. Kumawat, U. Rani, G. Arora, A.S. Verma, Ab-initio calculations of structural, optoelectronic, thermoelectric, and thermodynamic properties of mixed-halide perovskites RbPbBr 3−xIx (x = 0 to 3): applicable in renewable energy devices. ECS J. Solid State Sci. Technol. **12**, 083006 (2023)
11. T.K. Joshi, G. Sharma, R. Agarwal, A.S. Verma, Emerging potential photovoltaic absorber hybrid halide perovskites ($CH_3CH_2NH_3PbX_3$; X = Br, Cl) materials: an ab-initio calculation. Int. J. Energy Res. **45**, 13442–13460 (2021)
12. U. Rani, P.K. Kamlesh, T.K. Joshi, S. Sharma, R. Gupta, S.A.S. Verma, Alkaline earth based antiperovskite AsPX3 (X= Mg, Ca, and Sr) materials for energy conversion efficient and thermoelectric applications. Phys. Scripta **98**, 075902 (2023)
13 U. Rani, P.K. Kamlesh, T.K. Joshi, R. Singh, S. Sharma, R. Gupta, T. Kumar, A.S. Verma, Computational investigation of inverse perovskite $SbPX_3$ (X= Mg, Ca, and Sr) structured materials with applicability in green energy resources. Comput. Condensed Matter **36**, e00835 (2023)
14. U. Rani, P.K. Kamlesh, R. Agrawal, A. Shukla, A.S. Verma, Emerging study on lead-free hybrid double perovskite (CH3NH3)2AgInBr 6: potential material for energy conversion between heat and electricity. Energy Technol. **10**, 2200002 (2022)
15. J.K. Bairwa, P.K. Kamlesh, U. Rani, R. Singh, R. Gupta, S. Kumari, T. Kumar, A.J. Verma, Highly efficient and stable Ra_2LaNbO_6 double perovskite for energy conversion device applications. Mater. Sci. Energy Technol. **7**, 61–72 (2024)
16. M.A. Ali, R. Ullah, S. Murad, S.A. Dar, A. Khan, G. Murtaza, A. Laref, Insight into pressure tunable structural, electronic and

optical properties of $CsYbBr_3$ via DFT calculations. Eur Phys. J. Plus **135**, 309 (2020)
17. A.V. Nemtsev, V.S. Zhandun, V.I. Zinenko, Ab initio study of the polarization, electronic, magnetic, and optical properties of perovskite $SrMO_3$ (M = Fe, Mn) crystals and thin films containing magnetic ions. J. Exp. Theor. Phys. **126**, 497 (2018)
18. M. Sk, S. Ghosh, 16.35 % efficient Cs2GeSnCl6 based heterojunction solar cell with hole-blocking SnO2 layer: DFT and SCAPS-1D simulation. Optik Int. J. Light Electron Opt. **267**, 169608 (2022)
19. A.M. Mebed, S. Al-Qaisi, M.A. Ali, Study of optoelectronic and thermoelectric properties of double perovskites Rb_2AgBiX_6 (X = Br, I): by DFT approach. Eur Phys. J. Plus **137**, 990 (2022)
20. Y. Chrafih, M. Al-Hattab, K. Rahmani, Thermodynamic, optical, and morphological studies of the Cs_2AgBiX_6 double perovskites (X = Cl, Br, and I): insights from DFT study. J. Alloys Compd. **960**, 170650 (2023)
21. J.A. Abraham, D. Behara, K. Kumari, A. Srivastava, R. Sharma, S.K. Mukherjee, A comprehensive DFT analysis on structural, electronic, optical, thermoelectric, SLME properties of new double perovskite oxide Pb_2ScBiO_6. Chem Phys. Lett. **806**, 139987 (2022)
22. S. Alnujaim, A. Bouhemadou, M. Chegaar, A. Guechi, S. Bin-Omran, R. Khenata, Y. Al-Douri, W. Yang, H. Lu, Density functional theory screening of some fundamental physical properties of $Cs_2InSbCl_6$ and $Cs_2InBiCl_6$ double perovskites. Eur. Phys. J. B **95**, 114 (2022)
23. Y. Jain, S.S. Muneersab, D. Shrivastava, R. Kurchania, "Structural, mechanical, electronic, vibrational and thermoelectric properties of novel double perovskites Ba_2MgPdO_6 and Ba_2MgPtO_6 within DFT framework. Mater. Sci. Semicond **158**, 107381 (2023)
24. H. Absike, N. Baaalla, R. Lamouri, H. Labrim, H. Ez-zahraouy, Optoelectronic and photovoltaic properties of Cs_2AgBiX_6 (X = Br, Cl, or I) halide double perovskite for solar cells: insight from density functional theory. Int. J. Energy Res. **46**, 11053 (2022)
25. E. Haque, M.A. Hossain, Origin of ultra-low lattice thermal conductivity in Cs2BiAgX6 (X=Cl, Br) and its impact on thermoelectric performance. J. Alloys Compd. **748**, 63 (2018)
26. V.K. Ravi, N. Singhal, A. Nag, Initiation and future prospects of colloidal metal halide double-perovskite nanocrystals: Cs2AgBiX6 (X = Cl, Br, I). J. Mater. Chem. A **6**, 21666 (2018)
27. X. Zhou, J. Jankowska, H. Dong, O.V. Prezhdo, Recent theoretical progress in the development of perovskite photovoltaic materials. J. Energy Chem. **27**, 637 (2018)
28. W. Shi, T. Cai, Z. Wang, O. Chen, The effects of monovalent metal cations on the crystal and electronic structures of Cs_2MBiCl_6(M = Ag, Cu, Na, K, Rb, and Cs) perovskites. J. Chem. Phys. **153**, 141101 (2020)
29 M.A. Ali, A.A. Alothman, M. Mushab, A. Khan, M. Faizan, DFT Insight into structural, electronic, optical and thermoelectric properties of eco-friendly double perovskites Rb_2GeSnX_6 (X = Cl, Br) for green energy generation. J Inorg Organomet Polym (2023). https://doi.org/10.1007/s10904-023-02777-8
30. E.T. McClure, M.R. Ball, W. Windl, P.M. Woodward, Cs_2AgBiX_6 (X = Br, Cl): New visible light absorbing, lead-free halide perovskite semiconductors. Chem. Mater. **28**, 1348–1354 (2016)
31 S. Berri, N. Bouarissa, Density functional theory calculations of electronic structure and thermoelectric properties of K-based double perovskite materials. Energy Storage **5**, e400 (2023)
32. D. Behera, S.K. Mukherjee, First-principles calculations to investigate structural, optoelectronics and thermoelectric properties of lead free Cs_2GeSnX_6 (X = Cl, Br). Mater. Sci. Eng. B **292**, 116421 (2023)
33. P. Blaha, K. Schwarz, P. Sorantin, S.B. Trickey, Full-potential, linearized augmented plane wave programs for crystalline systems. Comput. Phys. Commun. **59**, 399 (1990)
34. P. Hohenberg, W. Kohn, Inhomogeneous electron gas. Phys. Rev. **136**, B864 (1964)
35. J.P. Perdew, K. Burke, Y. Wang, Generalized gradient approximation for the exchange-correlation hole of a many-electron system. Phys. Rev. B **54**, 16533 (1996)
36. F. Tran, P. Blaha, Accurate band gaps of semiconductors and insulators with a semilocal exchange-correlation potential. Phys. Rev. Lett. **102**, 226401 (2009)
37. G.K.H. Madsen, D.J. Singh, BoltzTraP: a code for calculating band-structure dependent quantities. Comput. Phys. Commun. **175**, 67 (2006)
38. S.J. Clark, M.D. Segall, C.J. Pickard, P.J. Hasnip, M.J. Probert, K. Refson, M.C. Payne, First principles methods using CASTEP. Crystall Mater. **220**, 567–570 (2005)
39. S.S. Essaoud, A. Bouhemadou, M.E. Ketfi, D. Allali, S. Bin-Omran, Structural parameters, electronic structure and linear optical functions of $LuXCo_2Sb_2$ (X = V, Nb and Ta) double half Heusler alloys. Physica B **657**, 414809 (2023)
40. M.A. Ali, A.A.A. Bahajjaj, S. Al-Qaisi, M. Sillanpaa, A. Khan, X. Wang, Structural, electronic, magnetic and thermoelectric properties of Tl_2NbX_6 (X = Cl, Br) variant perovskites calculated via density functional theory. J. Comput. Chem. **44**, 1875 (2023)
41 S.S. Essaoud, A. Bouhemadou, S. Maabed, S. Bin-Omran, R. Khenata, Pressure dependence of the electronic, optical, thermoelectric, thermodynamic properties of CsVO3: first-principles study. Phil. Magaz. **102**, 1522 (2022)
42. J. Singh, T. Kaur, A.P. Singh, M. Goyal, K. Kaur, S.A. Khandy, I. Islam, A.F. Wani, R. Krishan, M.M. Sinha, S.S. Verma, LiNbCoX (X = Al, Ga) quaternary Heusler compounds for high-temperature thermoelectric properties: a computational approach. Bull. Mater. Sci. **46**, 103 (2023)
43 F.D. Murnaghan, The compressibility of media under extreme pressures. Proc. Natl. Acad. Sci. USA **30**, 244–247 (1944)
44. M. Manzoor, M.W. Iqbal, N.A. Noor, H. Ullah, R. Sherma, S.S. Alarfaji, Exploring the structural, electronic, optical, and thermoelectric properties of potassium-based double perovskites K_2AgXI_6 (X = Sb, Bi) compounds: a DFT study. Mater. Sci. Eng. B **237**, 116122 (2023)
45. M. Gajdoš, K. Hummer, G. Kresse, J. Furthmüller, F. Bechstedt, Linear optical properties in the projector-augmented wave methodology. Phys. Rev. B—Condens. Matter Mater. Phys. **73**, 045112 (2006)
46. D. Bensaid, B. Doumi, S. Ahmad, Lithium doping effect for enhancing thermoelectric and optoelectronic performance of Co_2NbAl. JETP Lett. **115**, 539 (2022)
47. S. Galliano, F. Bella, M. Bonomo, G. Viscardi, C. Gerbaldi, G. Boschloo, C. Barolo, Hydrogel electrolytes based on xanthan gum: green route towards stable dye-sensitized solar cells. Nanomaterials **10**, 1585 (2020)
48. M.H. Ali, M.J. Islam, A. Kumer, M.S. Hossain, U. Chakma, D. Howlader, M.T. Islam, T. Hossain, Investigation of structural, electronic and optical properties of $Na_2InAgCl_6$, $K_2InAgCl_6$, and $Rb_2InAgCl_6$ lead-free halide double perovskites regarding with $Cs_2InAgCl_6$ perovskites cell and a comparative study by DFT Functionals. Mater. Res. **24**, e20210086 (2021)
49. M.A. Blanco, E. Francisco, V. Luania, GIBBS: isothermal-isobaric thermodynamics of solids from energy curves using a quasi-harmonic Debye model. Comput. Phys. Commun. **158**, 57 (2004)
50. G.A. Slack, Nonmetallic crystals with high thermal conductivity. J. Phys. Chem. Solids **34**, 321 (1973)
51 S.A. Mir, D.C. Gupta, Structural and mechanical stabilities, electronic, magnetic and thermophysical properties of double perovskite Ba_2LaNbO_6: Probed by DFT computation. Int J Energy Res. **45**, 14603 (2021)
52. S. Dahbi, N. Tahiri, O. El Bounagui, H. Ez-Zahraouy, Electronic, optical, and thermoelectric properties of perovskite $BaTiO_3$

compound under the effect of compressive strain. Chem Phys. **544**, 111105 (2021)